SUBPIXEL TARGET DETECTION IN HYPERSPECTRAL IMAGERY USING PIECE-WISE CONVEX SPATIAL-SPECTRAL UNMIXING, POSSIBILISTIC AND FUZZY CLUSTERING, AND CO-REGISTERED LIDAR

Taylor Glenn, Dmitri Dranishnikov, Paul Gader

University of Florida
Computer & Information Science & Engineering
Gainesville, FL 32611

Alina Zare

University of Missouri
Electrical & Computer Engineering
Columbia, MO 65211

ABSTRACT

A new algorithm for subpixel target detection in hyperspectral imagery is proposed which uses the PFCM-FLICM-PCE algorithm to model and estimate the parameters of the image background. This method uses the piece-wise convex mixing model with spatial-spectral constraints, and uses possibilistic and fuzzy clustering techniques to find the piece-wise convex regions and robustly estimate the parameters. A method for integrating the elevation measurements of a co-registered LiDAR sensor is also proposed. The performance of the proposed methods is demonstrated on a real-world dataset with emplaced detection targets.

Index Terms— hyperspectral imaging, lidar, detection, context-dependent, piece-wise convex

1. INTRODUCTION

Subpixel target detection in hyperspectral imagery (HSI) is a challenging problem and an area of active research. This paper proposes an advancement to subpixel target detection through the use of a more physically accurate data model as well as a robust background estimation technique. It also proposes a method to integrate co-registered LiDAR elevation measurements and evaluates the inclusion of LiDAR for improvements in performance.

The Neyman-Pearson lemma states that for a given set of model hypotheses, the likelihood ratio test will provide the optimal detection algorithm. When parameters of the model are unknown, they can be filled in with estimates. The generalized likelihood ratio test (GLRT) performed with these estimates loses optimality guarantees but still creates detectors that have been shown to work well. Most commonly used detectors such as the Spectral Matched Filter (SMF), Adaptive Cosine Estimator (ACE), and the Adaptive Matched Subspace Detector (AMSD) are formulated under the GLRT [1].

Given the framework of the GLRT, detection algorithms are formulated by specifying the statistical model under target present and target absent hypotheses, and specifying a method to estimate the unknown parameters. Advancements in performance then come from specifying better models and from estimating the parameters more robustly.

Many common HSI detection algorithms used for subpixel targets derive from a GLRT but are not formulated under subpixel models. One detector that uses a subpixel model within the GLRT framework, however, is the Hybrid Subpixel Detector (HSD) [2] which assumes that pixels follow the linear mixing model.

The HSD also assumes that the endmembers within the image are known a-priori, and that only abundances must be estimated to use the detector. In application however, endmembers are rarely known a-priori, and are often estimated from the image. An evaluation of various endmember estimation methods is given in [3].

The standard endmember estimation algorithms assume, however, that all pixels of the image are a convex combination of the same set of endmembers. The limitation of this assumption is that endmembers which are internal to the convex hull of the global image point cloud will not be discovered. For example, an image may have many regions of different character such as buildings, fields, and tree canopy; one or more of the endmembers of any given region, however, may lie inside the convex hull created by the entire image. Zare et al. have proposed a piece-wise convex model [4] and developed algorithms to find endmembers under the assumption of multiple convex regions [5, 6].

A recent development in this line of research is the PFCM-FLICM-PCE algorithm [7] which uses Possibilistic and Fuzzy clustering to estimate the endmembers under the assumption of multiple convex regions within the image. The fuzzy clustering is used to find the convex regions, while the possibilistic typicality weighting adds robustness to outliers in the estimation of the regions' endmembers and proportions. The algorithm also includes spatially constrained unmixing using the FLICM model [8], which encourages spatially neighboring pixels to have membership in the same convex region.

We propose a target detection algorithm which uses the

derivation and hypothesis test similar to the Hybrid Subpixel Detector, but uses the PFCM-FLICM-PCE algorithm for endmember estimation and unmixing. We further propose a method to integrate co-registered LiDAR elevation measurements to the PFCM-FLICM-PCE algorithm, and use the PFCM-FLICM-PCE-LIDAR method in a target detector. The following sections briefly outline the HSD detector and PFCM-FLICM-PCE algorithm and give an overview of our proposed detection approach.

2. PFCM-FLICM-PCE

The PFCM-FLICM-PCE algorithm is performed by an alternating optimization of the following objective function,

$$\begin{aligned} J =&(1-\alpha)\sum_{i=1}^{C}\sum_{j=1}^{N} a u_{ij}^{m}\left((\mathbf{x}_j-\mathbf{p}_{ij}\mathbf{E}_i)(\mathbf{x}_j-\mathbf{p}_{ij}\mathbf{E}_i)^T+G_{ij}\right)\\ &+b\,t_{ij}^{n}(\mathbf{x}_j-\mathbf{p}_{ij}\mathbf{E}_i)(\mathbf{x}_j-\mathbf{p}_{ij}\mathbf{E}_i)^T\\ &+a\sum_{i=1}^{C}(M\cdot\mathrm{trace}(\mathbf{E}_i\mathbf{E}_i^T)-\mathbf{1}_{1\times M}\mathbf{E}_i\mathbf{E}_i^T\mathbf{1}_{M\times 1}\\ &+\sum_{i=1}^{C}\gamma_i\sum_{j=1}^{N}(1-t_{ij})^n \end{aligned} \tag{1}$$

where a,b,α are tuning parameters of the algorithm, m is the fuzzifier for the fuzzy clustering, n is the parameter similar to a fuzzifier used for the typicalities, C is the specified number of convex regions, N is the number of pixels in the image, and M is the number of endmembers per convex region. The index $i=1\ldots,C$ runs over convex regions, and $j=1,\ldots,N$ runs over pixels in the image. The local spatial information term is given as

$$G_{ij}=\sum_{k\in N_j,\ k\neq j}\frac{1}{d_{jk}+1}(1-u_{ik})^m||\mathbf{x}_k-\mathbf{p}_{ik}\mathbf{E}_i||_2^2 \tag{2}$$

where d_{jk} is the distance in ground coordinates between pixel j and its neighbor pixel k within the local neighborhood N_j. The typicality scale term, γ_i, is set at each iteration to be the residual error of points to the convex region,

$$\gamma_i=\frac{1}{N}\sum_{j=1}^{N}||\mathbf{x}_j-\mathbf{p}_{ij}\mathbf{E}_i||_2^2 \tag{3}$$

The update equations for the endmembers matrices $\mathbf{E}_i$, proportion values $\mathbf{p}_{ij}$, memberships u_{ij}, and typicalities t_{ij} are given in the following equations:

$$\begin{aligned} \mathbf{E}_i=&\left(\sum_j(a u_{ij}^m+b\,t_{ij}^n)\mathbf{p}_{ij}^T\mathbf{p}_{ij}+2\alpha\mathbf{D}\right)^{-1}\\ &\times\left(\sum_j(a u_{ij}^m+b t_{ij}^n)\mathbf{p}_{ij}^T\mathbf{x}_j\right) \end{aligned} \tag{4}$$

where $\mathbf{D}=M\mathbf{I}_{M\times M}-\mathbf{1}_{M\times M}$

$$\mathbf{p}_{ij}^T = (\mathbf{E}_i\mathbf{E}_i^T)^{-1}(\mathbf{E}_i\mathbf{x}_j-\frac{\lambda_{ij}}{2}\mathbf{1}_{M\times 1}) \tag{5}$$

$$\lambda_{ij} = 2\frac{\mathbf{1}_{1\times M}(\mathbf{E}_i\mathbf{E}_i^T)^{-1}\mathbf{E}_i\mathbf{x}_j^T-1}{\mathbf{1}_{1\times M}(\mathbf{E}_i\mathbf{E}_i^T)^{-1}\mathbf{1}_{M\times 1}} \tag{6}$$

$$u_{ij} = \frac{1}{\sum_{q=1}^{C}\left(\frac{(\mathbf{x}_j-\mathbf{p}_{ij}\mathbf{E}_i)(\mathbf{x}_j-\mathbf{p}_{ij}\mathbf{E}_i)^T+G_{ij}}{(\mathbf{x}_j-\mathbf{p}_{qj}\mathbf{E}_q)(\mathbf{x}_j-\mathbf{p}_{qj}\mathbf{E}_q)^T+G_{qj}}\right)^{\frac{1}{m-1}}} \tag{7}$$

$$t_{ij} = \frac{1}{1+\left(\frac{b}{\gamma_i}||\mathbf{x}_j-\mathbf{p}_{ij}\mathbf{E}_i||_2^2\right)} \tag{8}$$

2.1. Hybrid Subpixel Detector

The Hybrid Subpixel Detector (HSD) starts with the following model hypotheses,

$$\begin{aligned} H_0 &: \mathbf{x}\sim\mathcal{N}(\mathbf{B}\mathbf{a}_{b,0},\sigma_0^2\Sigma)\\ H_1 &: \mathbf{x}\sim\mathcal{N}(\mathbf{S}\mathbf{a}_s+\mathbf{B}\mathbf{a}_{b,1}=\mathbf{E}\mathbf{a},\sigma_1^2\Sigma) \end{aligned} \tag{9}$$

and is then derived using the GLRT framework. The unknown endmembers, abundances and noise covariance parameters must be estimated. In this work the SPICE algorithm [9] is used to find endmembers and abundances, and the sample covariance of the image is used for the noise covariance. Given the estimates of the parameters, the resulting detection statistic is,

$$r_{\mathrm{HSD}}(\mathbf{x})=\frac{(\mathbf{x}-\mathbf{B}\hat{\mathbf{a}}_b)^T\Sigma^{-1}(\mathbf{x}-\mathbf{B}\hat{\mathbf{a}}_b)}{(\mathbf{x}-\mathbf{E}\hat{\mathbf{a}})^T\Sigma^{-1}(\mathbf{x}-\mathbf{E}\hat{\mathbf{a}})} \tag{10}$$

3. PROPOSED DETECTOR AND LIDAR INTEGRATION

The proposed detector is created through the following steps:

1. Use PFCM-FLICM-PCE to find background endmember sets $\mathbf{E}_i$, convex region memberships u_{ij}, and typicalities t_{ij}.
2. Add the target signature to each endmember set creating $\mathbf{S}_i=[s\ \mathbf{E}_i]$, then find new proportions $\mathbf{p}_{ij}^{(s)}$, memberships $u_{ij}^{(s)}$, and typicalities $t_{ij}^{(s)}$ using the PFCM-FLICM-PCE update equations.
3. Compute fuzzy and possibilistic weighted means $\hat{\boldsymbol{\mu}}_i$ and covariances $\hat{\boldsymbol{\Sigma}}_i$ for each class using equations (11),(12).

$$\hat{\boldsymbol{\mu}}_i = \frac{1}{\sum_{j=1}^{N}u_{ij}^m t_{ij}^n}\sum_{j=1}^{N}u_{ij}^m t_{ij}^n x_j \tag{11}$$

$$\hat{\boldsymbol{\Sigma}}_i = \frac{1}{\sum_{j=1}^{N}u_{ij}^m t_{ij}^n}\sum_{j=1}^{N}u_{ij}^m t_{ij}^n(\mathbf{x}_j-\hat{\boldsymbol{\mu}}_i)(\mathbf{x}_j-\hat{\boldsymbol{\mu}}_i)^T \tag{12}$$

4. Compute the detection statistic for each pixel using equation (13)

$$r_{\text{Fuzzy}-\text{HSD}}(\mathbf{x}_j) = \sum_{i=1}^{C} u_{ij} \frac{(\mathbf{x}_j - \mathbf{p}_{ij}^T \mathbf{E}_i)^T \hat{\mathbf{\Sigma}}_i^{-1} (\mathbf{x}_j - \mathbf{p}_{ij}^T \mathbf{E}_i)}{(\mathbf{x}_j - \mathbf{p}_{ij}^{(s)T} \mathbf{S}_i)^T \hat{\mathbf{\Sigma}}_i^{-1} (\mathbf{x}_j - \mathbf{p}_{ij}^{(s)T} \mathbf{S}_i)} \quad (13)$$

To integrate LiDAR measurements, we augment the distance computation d_{ij} used in the membership update equation (7) to be a three dimensional Euclidean distance. The first two of the three dimensions come from the assigned UTM coordinates of the image pixels and the third from the elevation of the LiDAR first return. This weighting thus decreases the enforced similarity of pixels if they have differing elevation, which would be an indication that they are from different convex regions of the image.

4. EXPERIMENTAL RESULTS

Data were collected by an airborne imaging spectrometer producing seventy-two 9.5 nm bands from 367 to 1043 nm, geo-referenced to a $1.0\,\text{m} \times 1.0\,\text{m}$ grid and converted to reflectance. A co-located LiDAR sensor measured elevation and intensity. LiDAR measurements were registered to the same grid, producing digital elevation maps (DEMs) of the first and last return.

Images were acquired over the University of Southern Mississippi campus near Gulfport, Mississippi, USA. An RGB image and DEM are shown in Figure 1. The scene contains buildings, roads, automobiles, grass, sidewalks, trees, bushes, a beach, etc. Four colored calibration cloths are visible in the center of the scene.

Cloth swatches stretched over wooden frames were placed around the campus as detection targets. Four colors (named Brown, Dark Green, Vineyard Green, and Pea Green) and 3 sizes ($0.5\,\text{m} \times 0.5\,\text{m}$, $1.0\,\text{m} \times 1.0\,\text{m}$, and $3.0\,\text{m} \times 3.0\,\text{m}$) were used. A total of 57 targets were placed on the ground in open areas, in shadow, or partially or fully occluded by trees. Many of the larger targets span multiple regions (e.g. both under tree cover and in the open). Some are very occluded and probably not detectable. The 3 sizes create targets that are definitely sub-pixel, probably sub-pixel, or contain at least one pure pixel if un-occluded. A single pure image pixel from an un-occluded 3m target of each color was selected as a target signature.

For this experiment, three detection results were evaluated. As a performance baseline, the HSD detector was used with the global endmembers found by SPICE. Next the PFCM-FLICM-PCE algorithm was used to find fuzzy partitions and endmembers for each partition. The Fuzzy-HSD detector given in (13) was used on the results of the PFCM-FLICM-PCE run. Finally PFCM-FLICM-PCE with the LiDAR DEM used in the spatial term was run and the

(a) RGB

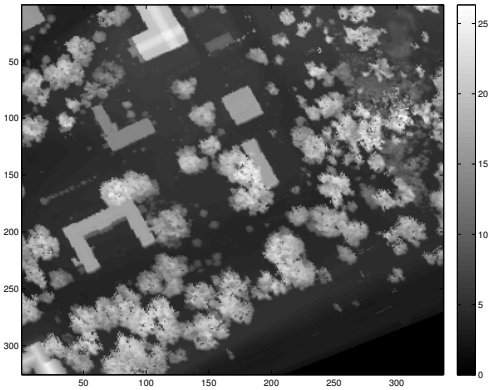

(b) LiDAR First Return DEM

Fig. 1. RGB and LiDAR DEM of Gulfport Dataset

Fuzzy-HSD was used on this output. For both the PFCM-FLICM-PCE and PFCM-FLICM-PCE-LIDAR runs the parameters were set to $C = 3$ convex regions, $M = 3$ endmembers per region, membership fuzzifier $m = 2$ and typicality fuzzifier $n = 1.5$, a 3×3 spatial neighborhood, $a = 20$, $b = 0.1$, and $\alpha = 0.001$. Both methods shared initialization values found by using Fuzzy C-means [10] clustering of the image spectra as initial partitions and then using VCA [11] to find initial endmembers in each region.

Results of the detection experiment are shown in Figure 2. The results are given as receiver operating characteristic (ROC) curves, which show the tradeoff of probability of detection (PD) versus false alarm rate (FAR) as the decision statistic threshold is varied over all confidence levels in the output. The range of false alarm rates used shows performance up to a reasonable upper limit for an operational system of 10^{-3} or 1 in 1000 pixels. In part (a) the ROCs show that using PFCM-FLICM-PCE method finds regions of distinct mixtures that are useful contextual information for target detection, with the Magenta curve exceeding the Red at nearly all false alarm rates. Using the LiDAR elevation information (Blue curve) further improves detection performance,

finding an additional target at the false alarm rate cutoff. Part (b) gives a zoomed in view of the same ROC curves with 95% confidence interval bands on the false alarm rates. Confidence intervals were estimated from a binomial fit to the number of observed false alarms at each PD out of the total number of opportunities (pixels) in the image. These intervals show that the proposed methods achieve detection rates of 0.49 at significantly lower false-alarm rates than the global method. They also show that the method using LiDAR achieves its highest detection levels at significantly better false alarm rates than without LiDAR.

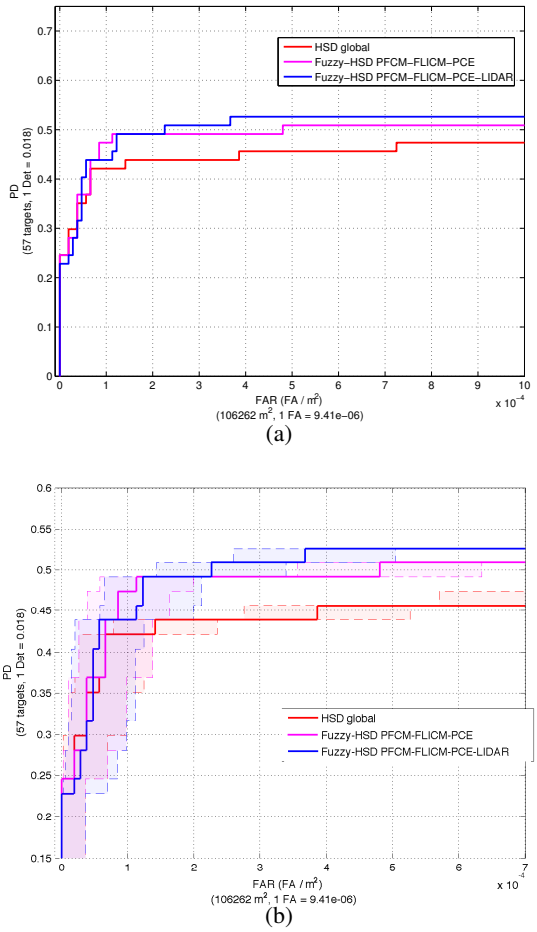

Fig. 2. ROCs without and with FAR 95% confidence interval bands

5. SUMMARY AND FUTURE WORK

We have presented a new method for sub-pixel target detection that uses piece-wise convex spatial-spectral unmixing, possibilistic and fuzzy clustering, and co-registered LiDAR information. The detection statistic is a fuzzy membership weighted version of the HSD detector. The experimental results indicate that the piece-wise convex model provides useful contextual information that improves subpixel detection performance over globally estimated endmembers and proportions. Additionally the use of LiDAR elevation information improves the contextual information so that detection performance is achieved at significantly better false-alarm rates. Future work will examine the performance of these methods on larger experiments. Additionally, while the PFCM-FLICM-PCE methods provide useful contextual information for detection, they are not optimized for that purpose. In future work, we plan to investigate joint optimization of the background estimation and the detector output.

6. REFERENCES

[1] D. Manolakis and G. Shaw, "Detection algorithms for hyperspectral imaging applications," *IEEE Signal Processing Magazine*, vol. 19, no. 1, pp. 29 –43, jan 2002.

[2] J. Broadwater and R. Chellappa, "Hybrid detectors for subpixel targets," *IEEE Transactions on Pattern Analysis and Machine Intelligence*, vol. 29, no. 11, pp. 1891 –1903, nov. 2007.

[3] A. Plaza, P. Martinez, R. Perez, and J. Plaza, "A quantitative and comparative analysis of endmember extraction algorithms from hyperspectral data," *IEEE Transactions on Geoscience and Remote Sensing*, vol. 42, no. 3, pp. 650 – 663, march 2004.

[4] A. Zare and P. Gader, "PCE: Piecewise convex endmember detection," *IEEE Transactions on Geoscience and Remote Sensing*, vol. 48, no. 6, pp. 2620 –2632, june 2010.

[5] A. Zare, P. Gader, O. Bchir, and H. Frigui, "Piecewise convex multiple-model endmember detection and spectral unmixing," *IEEE Transactions on Geoscience and Remote Sensing*, vol. PP, no. 99, pp. 1 –10, 2012.

[6] A. Zare, P. Gader, and G. Casella, "Sampling piecewise convex unmixing and endmember extraction," *IEEE Transactions on Geoscience and Remote Sensing*, vol. PP, no. 99, pp. 1 –11, 2012.

[7] A. Zare and P. Gader, "Piece-wise convex spatial-spectral unmixing of hyperspectral imagery using possibilistic and fuzzy clustering," in *Proceedings of 2011 IEEE International Conference on Fuzzy Systems*, june 2011, pp. 741 –746.

[8] A. Zare, "Spatial-spectral unmixing using fuzzy local information," in *Proceedings of 2011 IEEE International Geoscience and Remote Sensing Symposium (IGARSS)*, july 2011, pp. 1139 –1142.

[9] A. Zare and P. Gader, "Sparsity promoting iterated constrained endmember detection in hyperspectral imagery," *IEEE Geoscience and Remote Sensing Letters*, vol. 4, no. 3, pp. 446 – 450, july 2007.

[10] James C Bezdek, *Pattern recognition with fuzzy objective function algorithms*, Kluwer Academic Publishers, 1981.

[11] J.M.P. Nascimento and J.M. Bioucas Dias, "Vertex component analysis: a fast algorithm to unmix hyperspectral data," *IEEE Transactions on Geoscience and Remote Sensing*, vol. 43, no. 4, pp. 898–910, 2005.